OMTM, Volume *25*

Supplemental information

Pharmacological interventions enhance virus-free generation of *TRAC*-replaced CAR T cells

Jonas Kath, Weijie Du, Alina Pruene, Tobias Braun, Bernice Thommandru, Rolf Turk, Morgan L. Sturgeon, Gavin L. Kurgan, Leila Amini, Maik Stein, Tatiana Zittel, Stefania Martini, Lennard Ostendorf, Andreas Wilhelm, Levent Akyüz, Armin Rehm, Uta E. Höpken, Axel Pruß, Annette Künkele, Ashley M. Jacobi, Hans-Dieter Volk, Michael Schmueck-Henneresse, Renata Stripecke, Petra Reinke, and Dimitrios L. Wagner

Supplementary Information

Supplementary Table 1: DNA and protein sequences of different HDR template constructs (see Excel file).

Supplementary Table 2: Guide RNA target sequences (see Excel file).

Supplementary Table 3: HPRT1 HDR template and amplification primers (see Excel file).

Supplementary Table 4: Antibody information of flow cytometry panels (see Excel file).

Supplementary Figure 1:

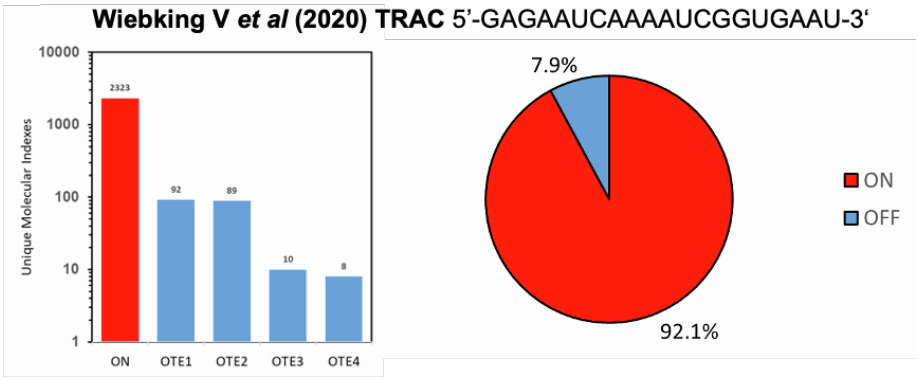

TRAC sgRNA (Wiebking 2020)	Reads	Target Sequence	Matched sequence (with highlighted mismatches to sgRNA)	Aligned sequence	Leveshtein distance	Chromo-some	Alignment start	Alignment stop	strand
On-target	2323	GAGAATCAAAATCGGTGAAT	GAGAATCAAAATCGGTGAAT	ATTCACCGATTTTGATTCTC	0	chr14	22547575	22547595	-
Off-target event 1	92	GAGAATCAAAATCGGTGAAT	TCTTATCAAAATCAGTGAAT	ATTCACTGATTTTGATAAGA	5	chr6	1112737	1112757	-
Off-target event 2	89	GAGAATCAAAATCGGTGAAT	GTGTATTTAAATTGTTTCAT	ATGAAACAATTTAAATACAC	8	chr1	237327485	237327505	-
Off-target event 3	10	GAGAATCAAAATCGGTGAAT	AAAAAACTAAATCAATTTAT	ATAAATTGATTTAGTTTTTT	8	chr22	34169261	34169281	-
Off-target event 4	8	GAGAATCAAAATCGGTGAAT	TATAATGAAAATTTAAAAAT	TATAATGAAAATTTAAAAAT	8	chr8	115314523	115314543	+

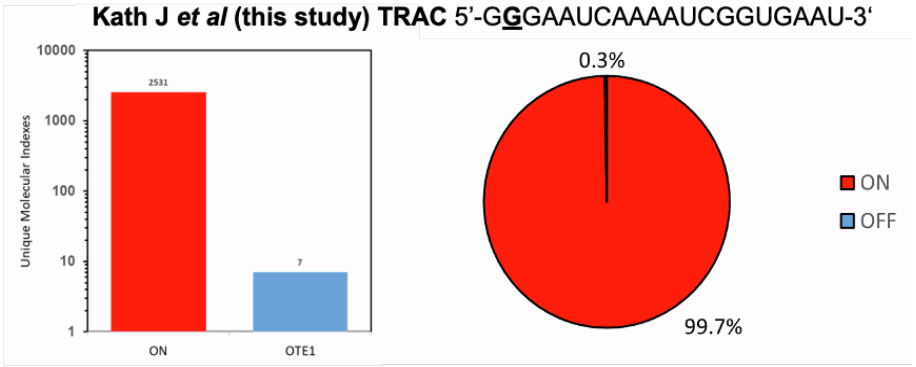

TRAC sgRNA (Charité)	Reads	Target Sequence	Matched sequence (with highlighted mismatches to sgRNA)	Aligned sequence	Leveshtein distance	Chromo-some	Alignment start	Alignment stop	strand
On-target	2531	GGGAATCAAAATCGGTGAAT	GAGAATCAAAATCGGTGAAT	ATTCACCGATTTTGATTCTC	1	chr14	22547575	22547595	-
Off-target event 1	7	GGGAATCAAAATCGGTGAAT	GGAAATATAAATTATTATAT	ATATAATAATTTATATTTCC	8	chr19	20782355	20782375	-

Suppl. Fig. 1: GUIDE-seq indicates reduced off-targets by target-sequence modified *TRAC* sgRNA. Results of GUIDE-seq analysis in HEK293 overexpressing SpCas9 for the original *TRAC* sgRNA (Wiebking *et al* 2020) and the sgRNA used in this study with the identified on- and off-target event locus sequences.

Supplementary Figure 2:

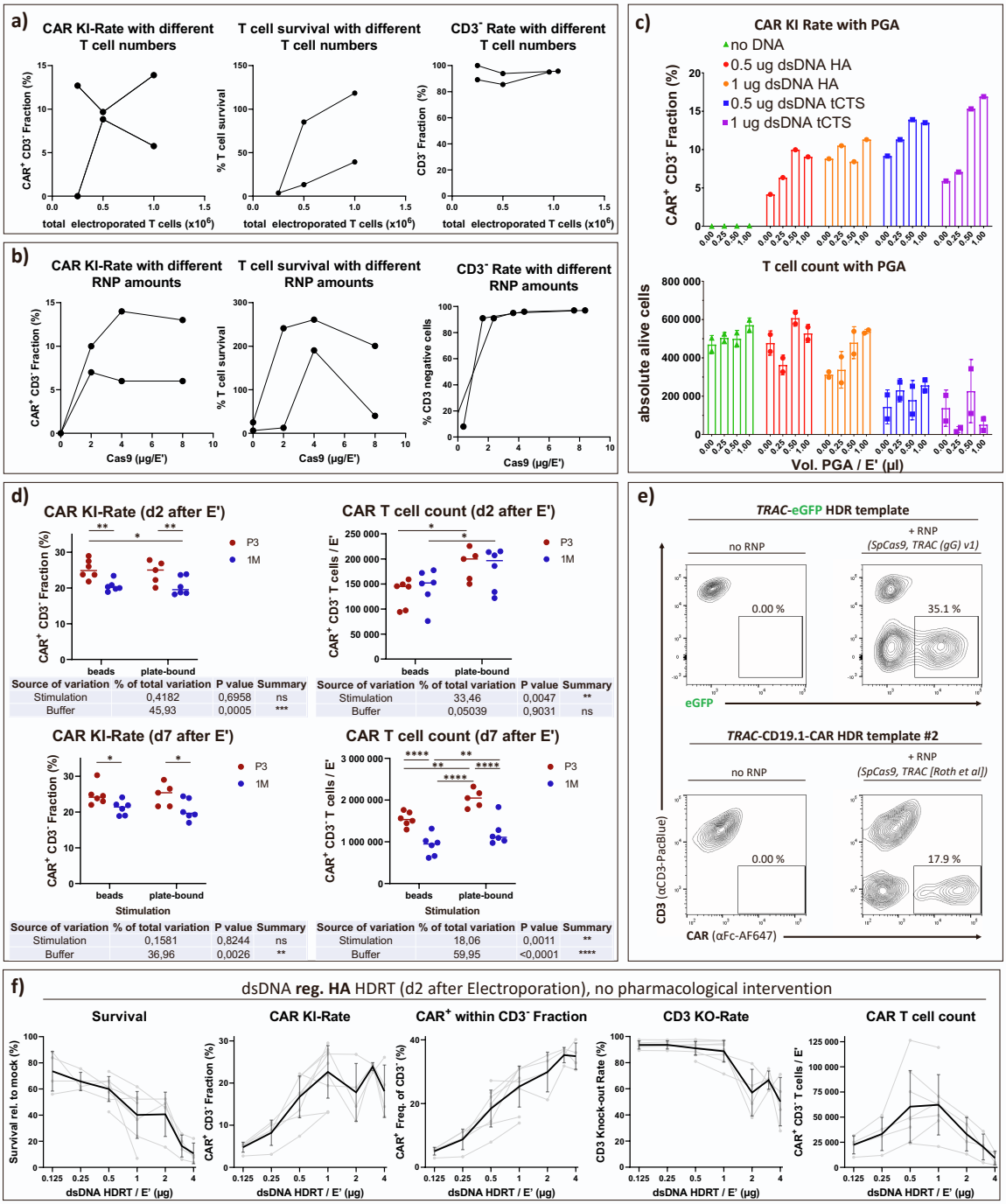

Suppl. Fig. 2: Optimization of electroporation parameters toward improved CAR T cell generation and cost reduction. (a) Effect of cell density during electroporation on CAR integration rates, relative survival compared to mock-electroporated cells, and CD3 knock-out rates as a marker of effective *TRAC* cutting (n = 2 donors). (b) Effect of RNP amount during electroporation. In contrast to other experiments, RNPs were pre-complexed with sgRNA at 2.5:1 molar ratio to SpCas9 (n = 2 donors). (c) Effect of poly-glutamic acid (PGA) on CAR integration rate and CAR T cell yield 4 days after electroporation (E'). RNPs were formulated by mixing 0.48 µl sgRNA (3.2 µg/µl) with the respective amount of PGA prior to adding 0.4 µl of Cas9 (10 µg/µl) (n = 2 technical replicates). (d) Effect of stimulation conditions and electroporation buffers on CAR knock-in rate and CAR T cell yield. (n = 2 donors in 3 techn. replicates). (e) Representative flow cytometry after electroporation with dsDNA HDR template alone or with co-delivered RNP. (f) Combined dataset of all dsDNA HDR-template titration experiments (for regular homology arm format) on day 2 after electroporation. (n = 5 donors in 3 independent experiments for titration between 0.25 and 1.0 µg; n = 4 donors in 2 independent experiments for titration between 0.5 and 4 µg HDRT / 20 µl electroporation volume.)

Supplementary Figure 3:

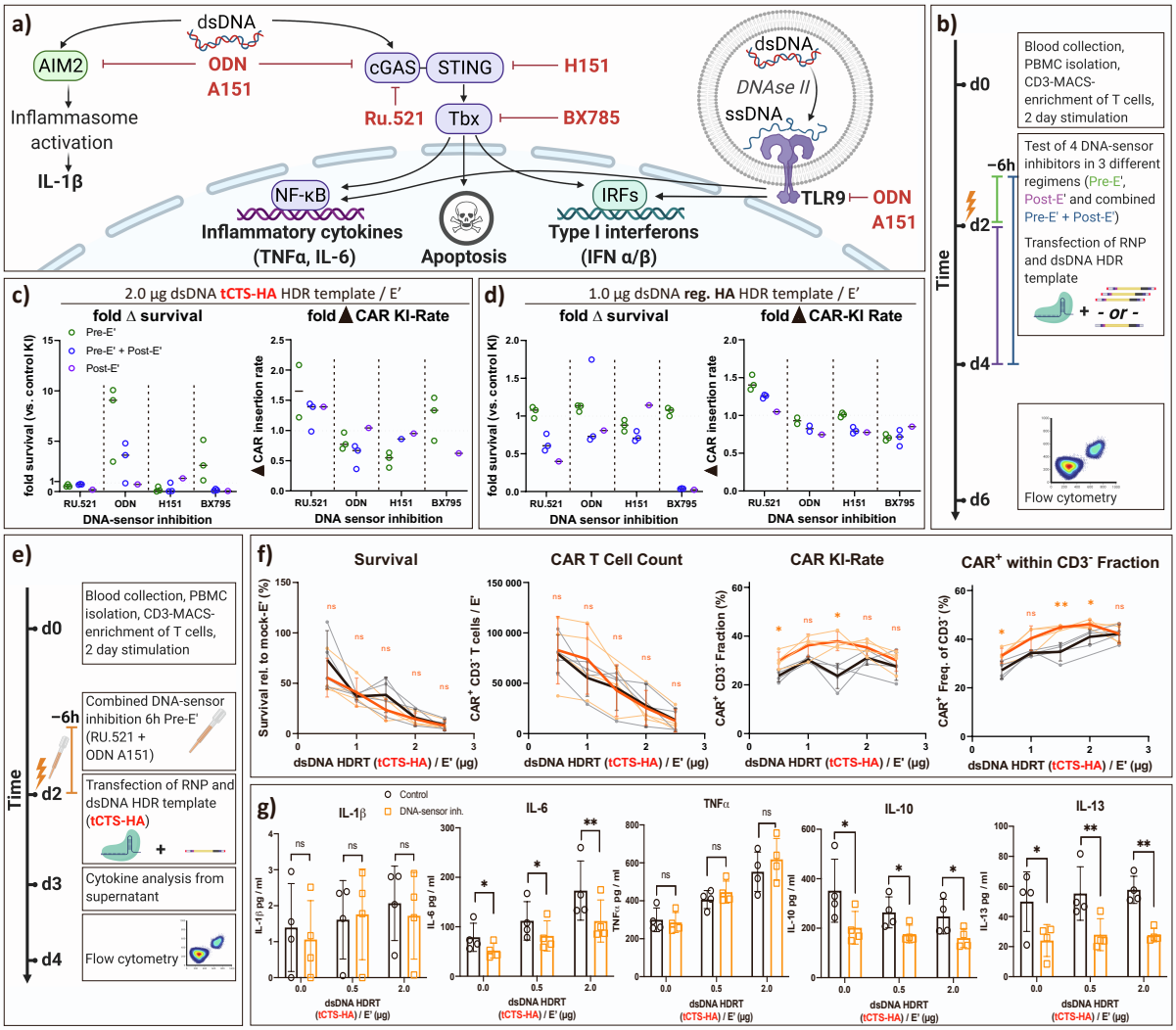

Suppl. Fig. 3: DNA sensor inhibition improves CAR T cell generation at high dsDNA concentrations. (a) Illustration of common DNA-sensing pathways as in **Fig. 2 a** with two additional inhibitors (BX785 and H151). (b) Experimental setup to evaluate transient DNA-sensor inhibition using 4 different compounds in 3 differently timed interventions. Green: drug is added 6 hours before electroporation. Purple: drug is present after electroporation for 48 hours. Blue: drug is present 6 hours before until 48 hours after electroporation. (c, d) Relative survival and CAR-detection rate after co-electroporation of T cells with RNP and high amount (2 µg / 20 ul electroporation volume) of tCTS-modified HDR template (c) or optimized dose (1 µg / 20 ul electroporation volume) of HDR template with regular HA (d). Both figures show the effects of differently timed interventions with each drug (n = 3 healthy donors). (e) Experimental setup for the combined ODN A151 + RU.521 treatment 6 hours prior to electroporation with RNP and escalating amounts of tCTS-HA modified dsDNA HDR template. (f) Summary of editing outcomes after combined DNA-sensor inhibition and electroporation with tCTS-HA HDRT (graphical representation as in **Fig. 2 c**; n = 4 donors in 2 independent experiments). Descriptive statistical analysis was performed using unpaired, two-tailed Student's t tests comparing values for no intervention with values for DNA-Sensor inhibition. (g) Summary of supernatant analysis for cytokines associated with DNA-sensing such as IL-1β (lower LOD: 0.85 pg/ml), IL-6 (lower LOD: 0.13 pg/ml) and TNFα (lower LOD: 0.05 pg/ml) as well as the Th2-associated cytokines IL-10 (lower LOD: 0.01 pg/ml) and IL-13 (lower LOD: 0.27 pg/ml) 24 hours after electroporation. Descriptive statistical analysis was performed using paired, two-tailed Student's t tests.

Supplementary Figure 4:

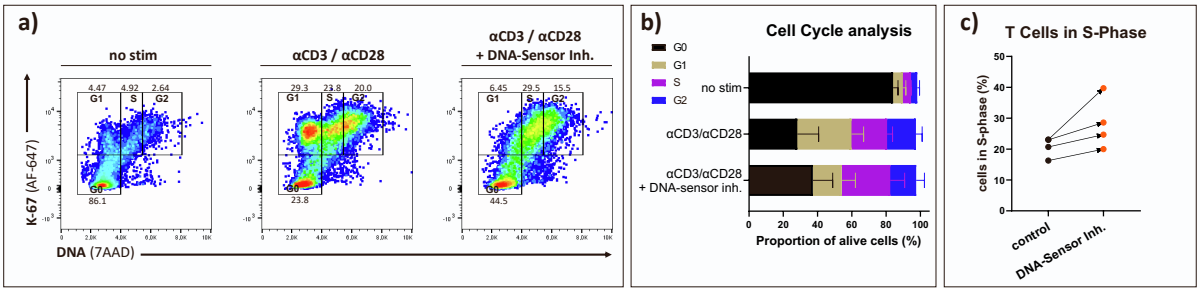

Suppl. Fig. 4: Cell cycle analysis after combined DNA-sensor inhibition indicates increased proportion of cells within S-phase. (a) Representative flow cytometry plots of a cell cycle staining (n = 4 donors in 2 independent experiments). Analysis of unstimulated T cells (left), anti-CD3/CD28 stimulated T cells (middle), and stimulated T cells after a combined 6-hour treatment with the DNA-sensor inhibitors RU.521 and ODN A151 (right). (b) Summary of **a**. (c) Summary of **a** for the impact of DNA-sensor inhibition on cells within S-phase.

Supplementary Figure 5:

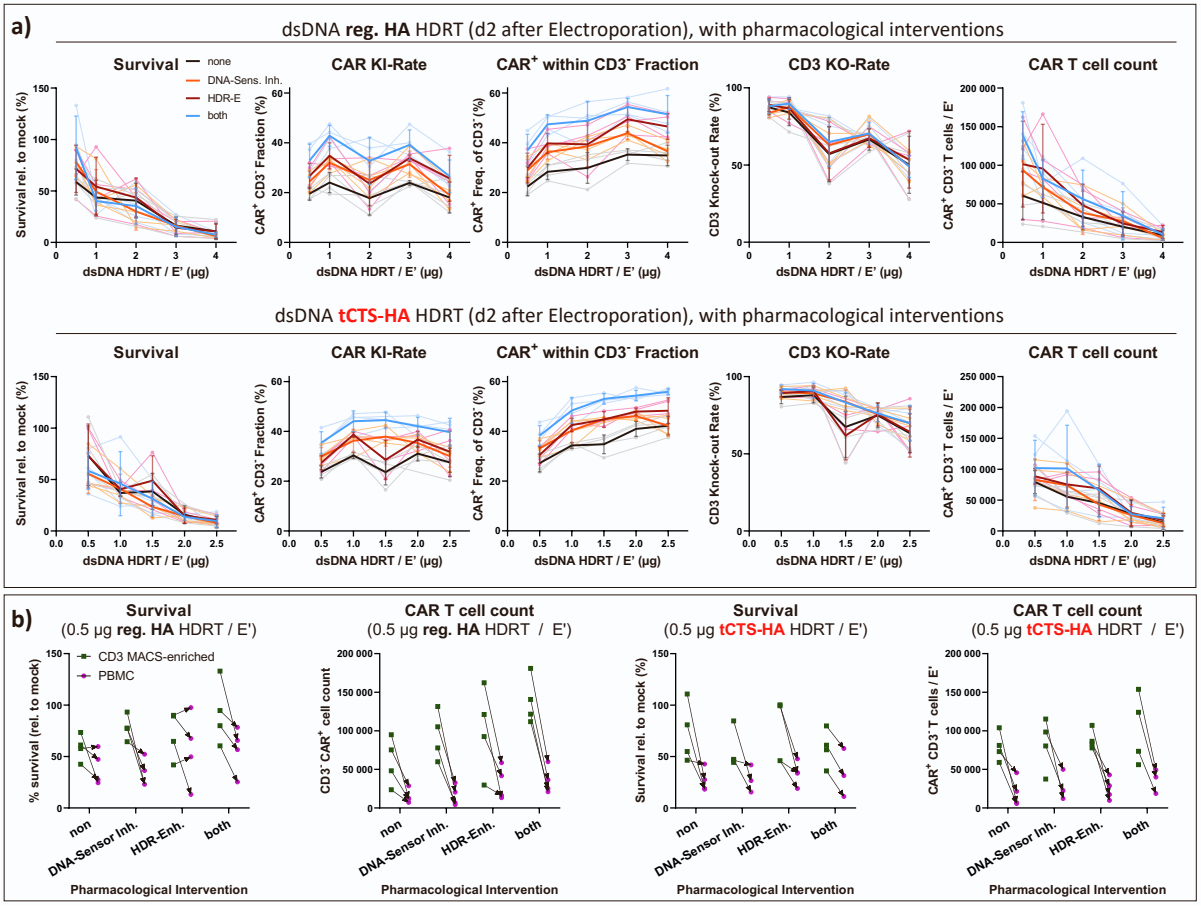

Suppl. Fig. 5: **HDR enhancers and DNA sensor inhibitors improve CAR T cell generation.** (a) Complete data set from experiments which were partially presented throughout this manuscript, including **Fig. 1 b-e**, **Fig. 2 c** and **Fig. 4 b**. These plots comprise the results of all tested parameters for both HDRT formats (reg. HA or tCTS-HA). Cells were analyzed by flow cytometry two days after electroporation (n = 4 donors in 2 independent experiments). (b) Comparison of PBMC and MACS-enriched CD3 cells as different starting material for CAR T cell generation for both HDRT formats. Cells were analyzed by flow cytometry two days after electroporation (n = 4 donors in 2 independent experiments).

Supplementary Figure 6:

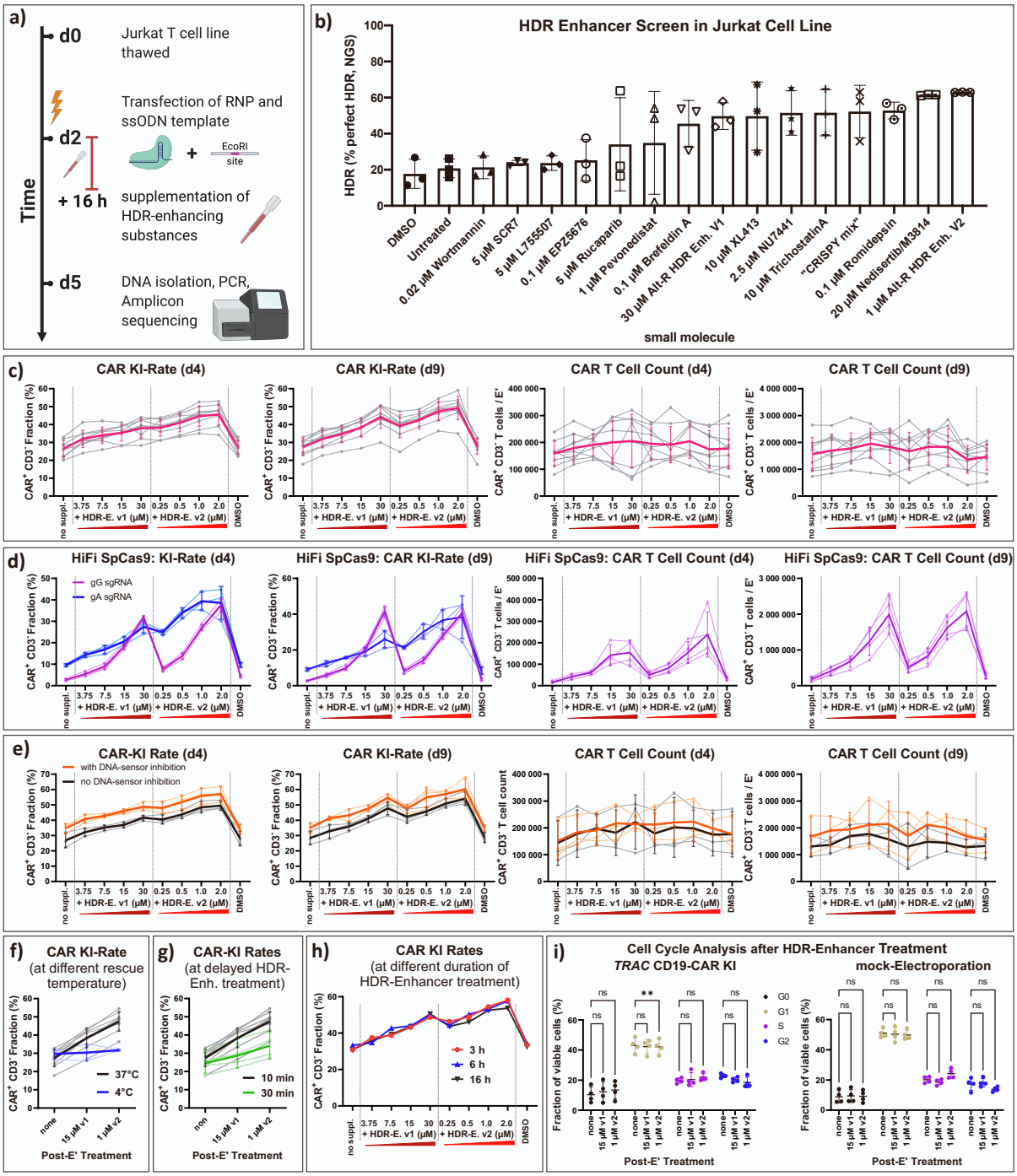

Suppl. Fig. 6: **Drug screen in Jurkat cells and subsequent testing in primary human T cells identifies another HDR-enhancing substance**. (a) Experimental setup to identify the effects of HDR enhancing substances on insertion rates of an exogenous DNA sequence motif (EcoRI restriction site, 6 bases) into the HPRT1 gene. (b) Summary of detected perfect HDR in genomic DNA of Jurkat T cells comparing different HDR-modulating small molecules. The "CRISPY MIX" drug cocktail was slightly modified to the original report and contained 30 µM NU7026, 10 µM Trichostatin A and 1 µM MLN4924. (n = 3 biol. replicates in 3 independent experiments). (c) Summary of full data set from knock-in experiments partially presented in **Fig. 3 a-c** testing the effects of Alt-R HDR enhancers V1 and V2 in primary human T cells. (n = 9 donors). (d) Similar experimental setup as **c**, here with Alt-R **HiFi** SpCas9 V3 as an alternative nuclease and 2 different sgRNAs (gG: '*TRAC* (gG) v1' and gA: '*TRAC* (Wiebking *et al*. 2020); (**Suppl. Table 2**)'. (n = 4 donors (gG) and 3 donors (gA)). (e) Titration of both Alt-R HDR enhancers with or without DNA-Sensor inhibition (n = 2 donors in 2 independent experiments). (f-h) Specific aspects of the HDR-enhancers' mode of action**.** (f) Temperature-dependent effects of HDR enhancers. Black lines represent conditions with T cell medium (+/- supplemented with HDR enhancers) pre-warmed to 37 °C (n = 9 donors). Blue lines represent conditions with 4 °C cold T cell medium (+/-

supplemented with HDR enhancers) at the time of cell transfer (n = 3 donors). (g) Time-sensitive effects of HDR enhancers. Editing outcomes of T cells subjected to a 30 min delay between electroporation (including immediate resuspension in T cell medium) and transfer into HDR enhancer supplemented T cell medium are shown in green (n = 4 donors). Controls (same as in **e**) are shown in black (n = 9 donors). (h) Effects of HDR enhancer treatment duration on editing outcomes. Half the supplemented medium was exchanged with drug-free T cell medium either 3, 6 or 16 hours post electroporation (n = 1 donor). (i) Cell cycle analysis of electroporated T cells with or without HDR-Enhancer treatment 16 hours after the electroporation.

Supplementary Figure 7:

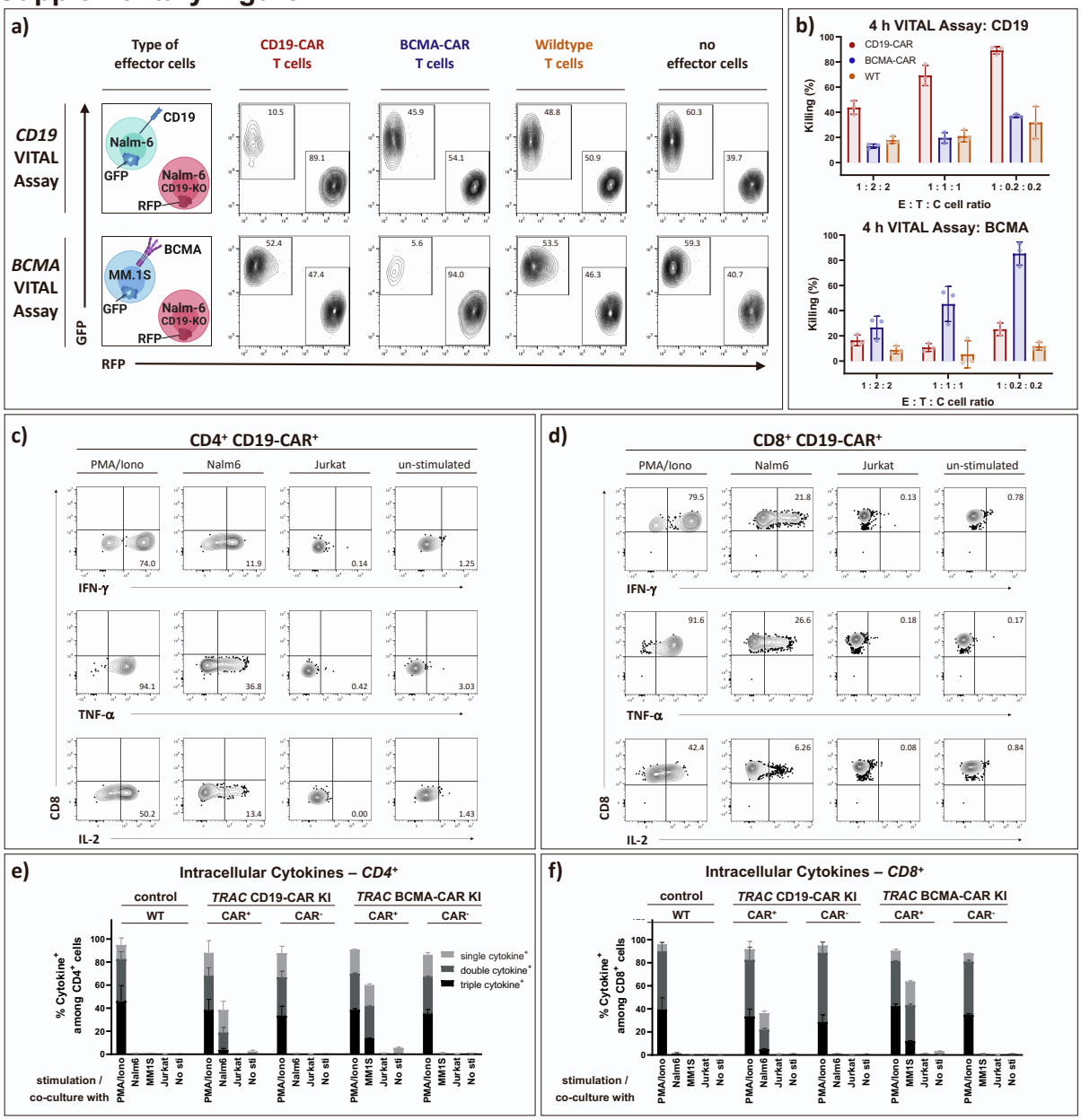

Suppl. Fig. 7: Virus-free generated *TRAC*-replaced CD19- and BCMA-specific CAR T cells exhibit comparable functionality *in vitro*. (a) 4 h VITAL Assay for CD19-CAR- and BCMA-CAR-mediated cytotoxicity. Representative flow cytometry plots show viable target (T) and control (C) cells after co-culture with respective effector (E) CAR T cells at E : T : C ratio of 1 : 0.2 : 0.2. Either Nalm-6 cells ($CD19^+$ $BCMA^-$, GFP^+; top) or MM.1S cells ($CD19^-$, $BCMA^+$, GFP^+; bottom) were used as the target cell population. CD19 knock-out RFP^+ Nalm-6 cells served as controls in both assays. (c) Summary of VITAL assays (n = 3 donors). (c, d) Intracellular cytokine staining of $CD4^+$ (e) or $CD8^+$ (f) (CAR) T cells after polyclonal stimulation with PMA/Ionomycin or co-culture with either $CD19^+$ Nalm-6 cells, $CD19^-$ Jurkat cells or $BCMA^+$ MM.1s cells. (e, f) Summary of intracellular cytokine staining as presented in **c** and **d**. Boolean gating was used to identify cells that produced one, two or three of the following cytokines: IFN-γ, IL-2 and TNFα. Error bars indicate standard deviation (n = 3 donors for wildtype T cells, 2 donors for TRAC CD19-CAR T cells and 1 donor for TRAC BCMA-CAR T cells; each biological replicate was assessed in technical duplicates).

Supplementary Figure 8:

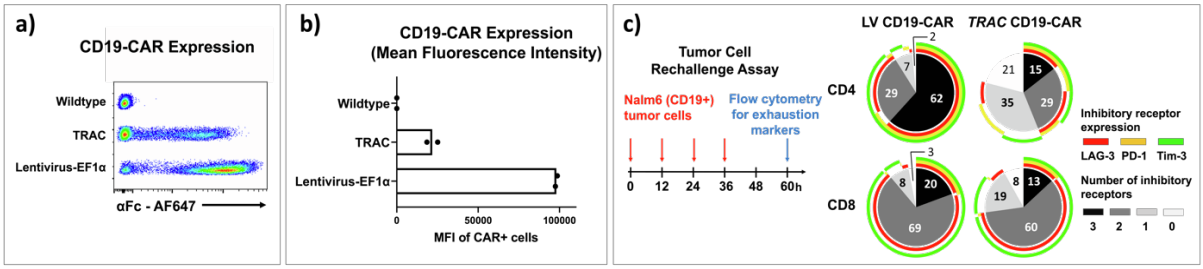

Suppl. Fig. 8: *TRAC*-replaced CD19-CAR T cells show reduced CAR expression and are less prone to exhaustion than lentiviral (LV) controls *in vitro*. (a, b) Comparison of CD19-CAR expression levels in CAR T cells generated by virus-free *TRAC*-integration or by LV gene transfer. (c) Expression of exhaustion markers on *TRAC*-replaced and LV CD19-CAR T cells after 4 rounds of co-culture with target Nalm-6 cells. The expression of individual inhibitory receptors per cell is indicated by colors. Different shades of grey relate to the number of inhibitory receptors per cell.

Supplementary Figure 9:

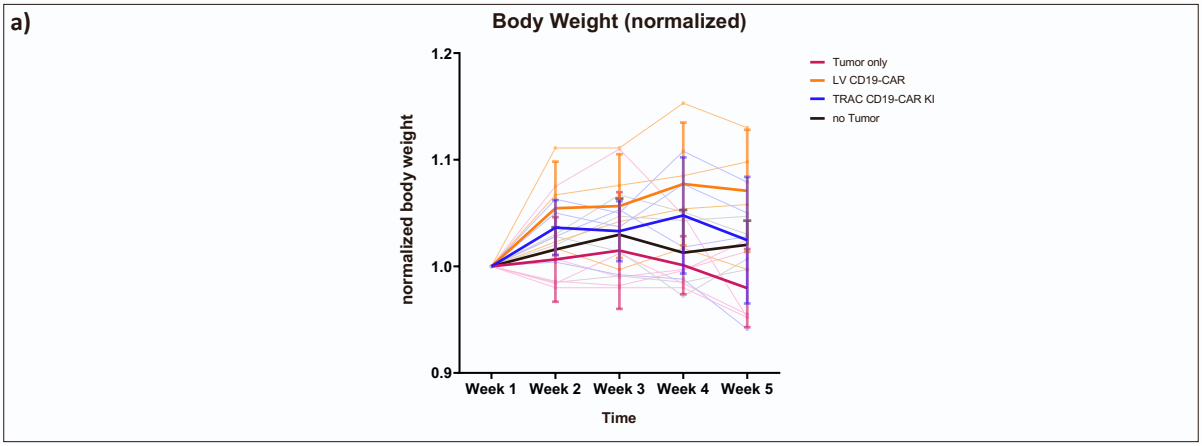

Suppl. Fig. 9: Normalized weight development of mice. Thin lines indicate the normalized body weight of each individual mouse. Thick lines indicate mean normalized body weight. Error bars indicate standard deviation.

Supplementary Figure 10:

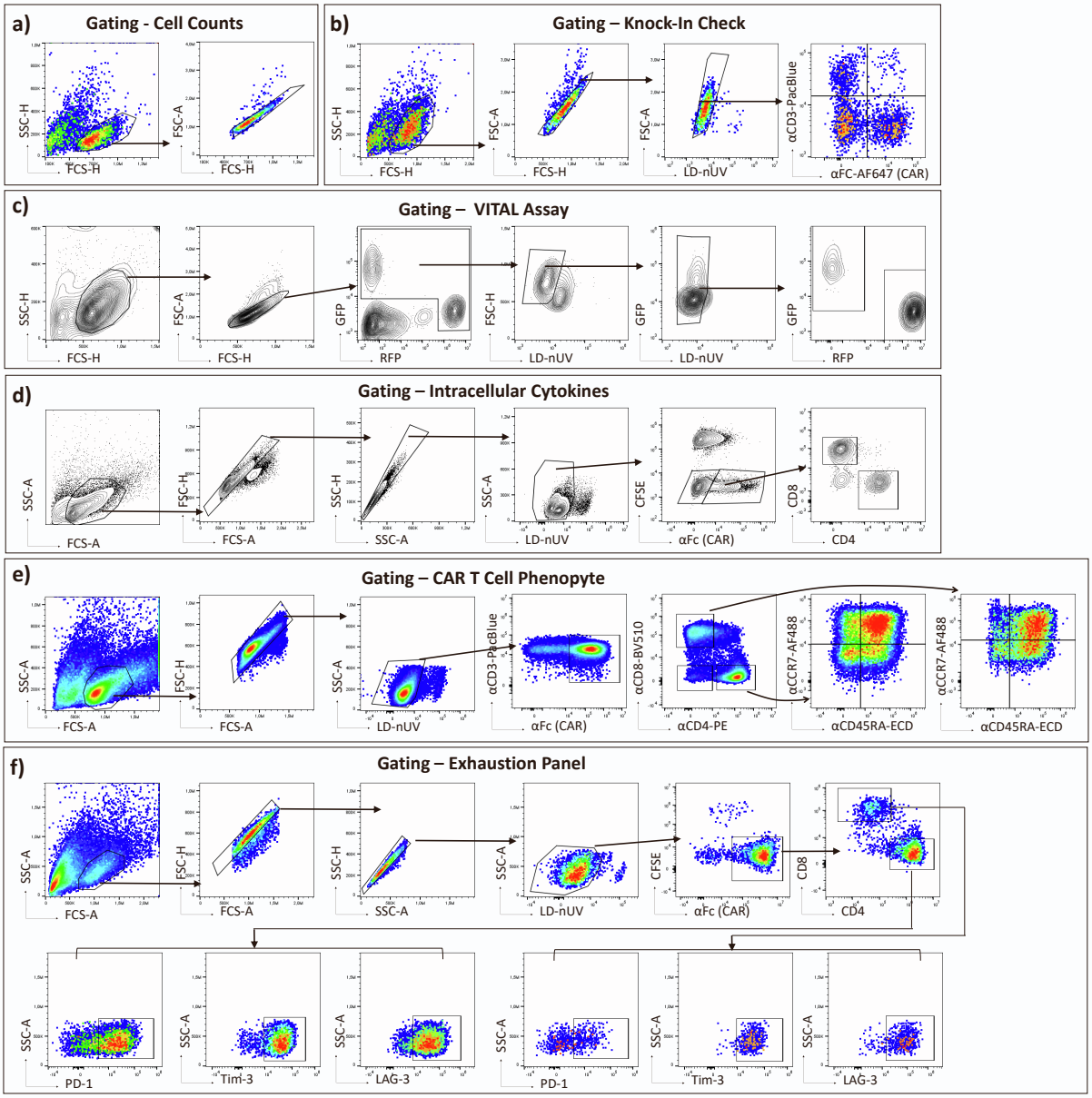

Suppl. Fig. 10: Representative gating strategies for flow cytometry analyses. (a) Gating for cell count determination. (b) Gating for analysis of editing outcomes ('Knock-In Check'). Such gating to identify TCR-replaced CAR T cells was applied in all experiments that did not require T cell stimulation or intracellular staining. (c) Gating strategy to determine target : control cell ratios for the VITAL assays (as presented in Fig. 8 b, c). (d) Gating after intracellular staining to determine cytokine production following different modes of (CAR) T cell stimulation (as presented in Fig. 8 e-h). (e) Gating strategy for phenotype assessment of (CAR) T cells (as presented in Suppl. Fig. 4 d).